International Journal of Electrical and Computer Engineering (IJECE)
Vol. 14, No. 6, December 2024, pp. 6351~6359
ISSN: 2088-8708, DOI: 10.11591/ijece.v14i6.pp6351-6359

Performance analysis of cascade spline adaptive filtering based on normalized orthogonal gradient adaptive algorithm

Theerayod Wiangtong[1], Suchada Sitjongsataporn[2]
[1]Department of Electrical Engineering, School of Engineering, King Mongkut's Institute of Technology Ladkrabang, Bangkok, Thailand
[2]Department of Electronic Engineering, Mahanakorn Institute of Innovation, Faculty of Engineering and Technology, Mahanakorn University of Technology, Bangkok, Thailand

Article Info

Article history:

Received May 14, 2024
Revised Jun 20, 2024
Accepted Aug 6, 2024

Keywords:

Cascade architecture
Linear adaptive filtering
Nonlinear system
Normalized orthogonal gradient adaptive algorithm
Spline adaptive filtering

ABSTRACT

In this paper, the cascade architecture of spline adaptive filtering (CSAF) for nonlinear systems is presented with the normalized version of orthogonal gradient adaptive (NOGA) algorithm. Spline adaptive filtering comprises a sandwich of the first linear adaptive filtering (LAF) and nonlinear adaptive look-up table. In this cascading architecture, SAF is connected to the second LAF. NOGA is considered as the fast convergence applied by stochastic gradient-based approach. Convergence properties of the proposed NOGA-CSAF algorithm in terms of instantaneous errors can be derived by using Taylor series expansion. Experimental results demonstrate the effectiveness of proposed NOGA-CSAF algorithm using the mean square error scheme. It clearly outperforms the traditional least mean square algorithm on CSAF model in the nonlinear identification system.

Corresponding Author:

Theerayod Wiangtong
Department of Electrical Engineering, School of Engineering, King Mongkut's Institute of Technology Ladkrabang
1 Chalong Krung 1 Alley, Lat Krabang, Bangkok 10520, Thailand
Email: theerayod.wi@kmitl.ac.th

1. INTRODUCTION

According to the practical situations, the nonlinear adaptive filtering (NAF) models are involved to guarantee for many field of real-world applications [1]–[4]. As stated in a linear-nonlinear (LN) architecture based on Wiener model [5]–[10], the spline-based adaptive filtering (SAF) architecture consists of linear adaptive filtering (LAF) connected to adaptive look-up table (LUT) for NAF adapted by spline-based interpolation. SAF has been investigated to against the impulsive or colored noise [8], [9]. In [9], [10], SAF-based architecture has been analyzed in the convergence properties by adaptive step-size mechanism. Based on Hammerstein function, the Hammerstein-based SAF (HSAF) has been derived by a nonlinear-linear (NL) model implemented to a block-oriented NAF connected with LAF approach [11]–[14]. Referring to HSAF model, there are many evaluations of performance in the various engineering field as presented in the ultrasonic motor system [15] and nonlinear digital cancellation in mode of full-duplex [16], [17].

A general trouble in nonlinear systems is that there is no "$a\ priori$" or previous information used. A set of the cascade of linear and nonlinear model has been introduced to identify the best solution with the present information in the real-world environment [18]–[21]. As stated in [19], [20], the cascade spline-based adaptive filtering (CSAF) consists of a nonlinear-linear-nonlinear (NLN) and a linear-nonlinear-linear (LNL) models with least mean square (LMS) algorithm that has been proposed in the system identification. In [20], a class of CSAF scheme has been investigated on the nonlinear radio system working at 2.4 GHz industrial, scientific, and medical (ISM) band to evaluate the self-interference in various scenarios. Meanwhile, the modified CSAF based on the normalized version of LMS (NLMS) algorithm [21] has been modified in the identification nonlinear system.

For the fast learning convergence, the adaptation of orthogonal gradient adaptive (OGA) mechanism in [22]–[24] can be furnished with the normalized version of OGA (NOGA) algorithm. In study [23], the convergence analysis of NOGA has been derived with the greedy scheme. In study [24], the orthogonal gradient descent algorithm has been proposed on neural networks in the areas of continual learning.

The contribution of this work is to derive the CSAF model using NOGA mechanism under the minimized cost function on stochastic gradient-based approach. To the best of our knowledge, the NOGA mechanism can guarantee the convergence rate by using the CSAF approach. Cascade architecture on SAF mechanism is detailed briefly in section 2. Based on NOGA algorithm, the adaptive directional and negative gradient vectors of NOGA are important keys for smooth and fast convergence as shown in section 3. Moreover, the convergence properties of proposed NOGA-CSAF algorithm are derived by using Taylor expansion in section 4. Section 5 presents some experimental results for the nonlinear identification dynamic system. Finally, section 6 concludes the work.

2. THE PROPOSED CASCADE SPLINE ARCHITECTURE BASED ON NORMALIZED ORTHOGONAL GRADIENT ADAPTIVE ALGORITHM

In [19], [21], the cascade or sandwich models are presented for nonlinear system identification. In this paper, the cascade of LNL model is considered as spline-based system, as shown in Figure 1. This cascade model comprises two LAFs and a nonlinear memoryless function in the middle. At the first block of LAF $\boldsymbol{w}_1(k)$, the output $z(k)$ is given by (1).

$$z(k) = \boldsymbol{w}_1(k)^T \boldsymbol{x}(k), \tag{1}$$

where $\boldsymbol{x}(k)$ denotes as the input vector.

Subsequently, the output vector $\boldsymbol{s}(k)$ of a NAF $\boldsymbol{m}_j(k)$ at the j^{th}-index span can be expressed by (2).

$$\boldsymbol{s}(k) = \boldsymbol{a}(k)^T \cdot \boldsymbol{D} \cdot \boldsymbol{m}_j(k), \tag{2}$$

where $\boldsymbol{D}$ is a spline basis matrix. It is noted that the weight vector $\boldsymbol{m}_j(k)$ works as the adaptive controlling vector for the third-order polynomial spline interpolation $\boldsymbol{a}(k)$ as (3).

$$\boldsymbol{a}(k) = [a(k)^3 \quad a(k)^2 \quad a(k) \quad 1]^T , \tag{3}$$

where $\boldsymbol{a}(k)$ is a local parameter that is calculated by (4).

$$a(k) = \frac{z(k)}{\sigma_x} - \left\lfloor \frac{z(k)}{\sigma_x} \right\rfloor \tag{4}$$

where σ_x is a space between 2-connected controlling taps. And a position of index span (j) for nonlinear adaptive controlling vector $\boldsymbol{m}_j(k)$ is related with the output $z(k)$ of the first linear adaptive weight vector $\boldsymbol{w}_1(k)$ and number of tap length (P) of $\boldsymbol{m}_j(k)$ as (5).

$$j = \left\lfloor \frac{z(k)}{\sigma_x} \right\rfloor + \left(\frac{P-1}{2} \right), \tag{5}$$

where $\lfloor \cdot \rfloor$ is a floor operator and P is a uniform degree spline interpolation. It is noted that a position j from (5) should be adjusted in the middle range of $\boldsymbol{m}_j(k)$. Therefore, the output $y(k)$ of the second LAF $\boldsymbol{w}_2(k)$ is given by (6).

$$y(k) = \boldsymbol{w}_2(k)^T \boldsymbol{s}(k). \tag{6}$$

As stated in [6], a nonlinear problem is no "$a\ priori$" information in general. So, the output error $\epsilon(k)$ from Figure 1 can be expressed as (7).

$$\epsilon(k) = d(k) - y(k) = d(k) - \boldsymbol{w}_2(k)^T \boldsymbol{s}(k), \tag{7}$$

where $d(k)$ denotes as a reference signal.

In this section, we introduce a NOGA-based algorithm on cascade spline-based architecture for nonlinear adaptive filtering. In studies [19], [21] the normalized version for squared error cost function $\mathcal{J}(\boldsymbol{w}_1, \boldsymbol{m}_j, \boldsymbol{w}_2)$ is considered by the instantaneous error in (8).

$$\mathcal{J}(\boldsymbol{w}_1, \boldsymbol{m}_j, \boldsymbol{w}_2) = \frac{1}{2}\left\{\frac{\epsilon(k)^2}{\boldsymbol{x}(k)^T\boldsymbol{x}(k)}\right\}, \tag{8}$$

where $\epsilon(k)$ is given in (7).

The adaptive learning algorithm can be derived to minimize the cost function in (8), based on stochastic gradient mechanism by computing the gradient with respect to (w.r.t.) the second LAF at (9).

$$\frac{\partial\mathcal{J}(\boldsymbol{w}_1,\boldsymbol{m}_j,\boldsymbol{w}_2)}{\partial\boldsymbol{w}_2(k)} = -\frac{\epsilon(k)}{\boldsymbol{x}(k)^T\boldsymbol{x}(k)}\frac{\partial y(k)}{\partial\boldsymbol{w}_2(k)} = -\frac{\epsilon(k)}{\boldsymbol{x}(k)^T\boldsymbol{x}(k)}\boldsymbol{s}(k). \tag{9}$$

For the adaptive controlling vector $\boldsymbol{m}_j(k)$, it is possible to obtain by (10).

$$\frac{\partial\mathcal{J}(\boldsymbol{w}_1,\boldsymbol{m}_j,\boldsymbol{w}_2)}{\partial\boldsymbol{m}_j(k)} = -\frac{\epsilon(k)}{\boldsymbol{x}(k)^T\boldsymbol{x}(k)}\cdot\frac{\partial y(k)}{\partial s(k)}\cdot\frac{\partial s(k)}{\partial\boldsymbol{m}_j(k)} = -\frac{\epsilon(k)}{\boldsymbol{x}(k)^T\boldsymbol{x}(k)}\,\boldsymbol{a}(k)^T\cdot\boldsymbol{D}\cdot\boldsymbol{w}_2(k). \tag{10}$$

For the derivation of stochastic mechanism for the first LAF $\boldsymbol{w}_1(k)$, it is possible to compute by (11).

$$\begin{aligned}\therefore\frac{\partial\mathcal{J}(\boldsymbol{w}_1,\boldsymbol{m}_j,\boldsymbol{w}_2)}{\partial\boldsymbol{w}_1(k)} &= -\frac{\epsilon(k)}{\boldsymbol{x}(k)^T\boldsymbol{x}(k)}\cdot\frac{\partial y(k)}{\partial s(k)}\cdot\frac{\partial s(k)}{\partial\boldsymbol{a}(k)}\cdot\frac{\partial\boldsymbol{a}(k)}{\partial\boldsymbol{w}_1(k)}\\ &= -\frac{\epsilon(k)}{\boldsymbol{x}(k)^T\boldsymbol{x}(k)}\,\boldsymbol{w}_2(k)^T\cdot\boldsymbol{D}\cdot\boldsymbol{\alpha}(k)\cdot\boldsymbol{m}_j(k)\cdot\frac{\boldsymbol{x}(k)}{\sigma_x},\end{aligned} \tag{11}$$

where $\boldsymbol{\alpha}(k)$ is derivation of $\boldsymbol{a}(k)$ defined by (12).

$$\boldsymbol{\alpha}(k) = [3a(k)^2 \quad 2a(k) \quad 1 \quad 0]^T, \tag{12}$$

where $[\cdot]^T$ is a transpose operator.

The proposed weight vector $\boldsymbol{w}_2(k)$ based on NOGA with the help of directional weight $\varphi_{w_2}(k)$ and gradient vector $\zeta_{w_2}(k)$ can be derived from (13) and (14).

$$\boldsymbol{w}_2(k+1) = \boldsymbol{w}_2(k) + \mu_{w_2}\cdot\varphi_{w_2}(k), \tag{13}$$

$$\varphi_{w_2}(k+1) = \varphi_{w_2}(k) - \gamma_{w_2}\cdot\zeta_{w_2}(k), \tag{14}$$

where μ_{w_2} and γ_{w_2} are the tuning value and forgetting-factor for $\boldsymbol{w}_2(k)$.

For the stochastic learning, the gradient $\zeta_{w_2}(k)$ for $\boldsymbol{w}_2(k)$ can be obtained by (15).

$$\zeta_{w_2}(k+1) = \gamma_{w_2}\cdot\zeta_{w_2}(k) + \frac{\partial\mathcal{J}(\boldsymbol{w}_1,\boldsymbol{m}_j,\boldsymbol{w}_2)}{\partial\boldsymbol{w}_2(k)}, \tag{15}$$

where $\frac{\partial\mathcal{J}(\boldsymbol{w}_1,\boldsymbol{m}_j,\boldsymbol{w}_2)}{\partial\boldsymbol{w}_2(k)}$ is given in (9). Therefore, the adaptive gradient $\zeta_{w_2}(k)$ can be performed by (16).

$$\zeta_{w_2}(k+1) = \gamma_{w_2}\cdot\zeta_{w_2}(k) - \frac{\boldsymbol{s}(k)\epsilon(k)}{\boldsymbol{x}(k)^T\boldsymbol{x}(k)}, \tag{16}$$

where γ_{w_2} lies upon the orthogonal projection of present directional weight $\varphi_{w_2}(k)$ and gradient $\zeta_{w_2}(k)$ as (17).

$$\gamma_{w_2} = \frac{\varphi_{w_2}(k)^T\cdot\zeta_{w_2}(k)}{\varphi_{w_2}(k+1)^T\cdot\varphi_{w_2}(k)}. \tag{17}$$

Similarly, the proposed spline-based controlling vector $\boldsymbol{m}_j(k)$ can be expressed on NOGA with the help of $\varphi_{m_j}(k)$ and $\zeta_{m_j}(k)$ as (18)-(20).

$$\boldsymbol{m}_j(k+1) = \boldsymbol{m}_j(k) + \mu_{m_j}\cdot\varphi_{m_j}(k), \tag{18}$$

$$\varphi_{m_j}(k+1) = \varphi_{m_j}(k) - \gamma_{m_j} \cdot \zeta_{m_j}(k), \quad (19)$$

$$\zeta_{m_j}(k+1) = \gamma_{m_j}\zeta_{m_j}(k) + \frac{\partial \mathcal{J}(\boldsymbol{w}_1, \boldsymbol{m}_j, \boldsymbol{w}_2)}{\partial \boldsymbol{m}_j(k)}, \quad (20)$$

where μ_{m_j}, γ_{m_j} are tuning and forgetting-factor respectively for $\boldsymbol{m}_j(k)$ and $\frac{\partial \mathcal{J}(\boldsymbol{w}_1, \boldsymbol{m}_j, \boldsymbol{w}_2)}{\partial \boldsymbol{m}_j(k)}$ is given in (10). Therefore, the gradient vector $\zeta_{m_j}(k)$ can be evaluated by (21), (22)

$$\zeta_{m_j}(k+1) = \gamma_{m_j}\zeta_{m_j}(k) - \frac{\boldsymbol{a}(k)^T \cdot \boldsymbol{D} \cdot \boldsymbol{w}_2(k)\epsilon(k)}{\boldsymbol{x}(k)^T \boldsymbol{x}(k)}, \quad (21)$$

$$\gamma_{m_j} = \frac{\varphi_{m_j}(k)^T \cdot \zeta_{m_j}(k)}{\varphi_{m_j}(k+1)^T \cdot \varphi_{m_j}(k)}. \quad (22)$$

Finally, the proposed linear vector $\boldsymbol{w}_1(k)$ based on NOGA in terms of $\varphi_{w_1}(k)$ and $\zeta_{w_1}(k)$ can be computed as (23)-(25).

$$\boldsymbol{w}_1(k+1) = \boldsymbol{w}_1(k) + \mu_{w_1} \cdot \varphi_{w_1}(k), \quad (23)$$

$$\varphi_{w_1}(k+1) = \varphi_{w_1}(k) - \gamma_{w_1} \cdot \zeta_{w_1}(k), \quad (24)$$

$$\zeta_{w_1}(k+1) = \gamma_{w_1} \cdot \zeta_{w_1}(k) + \frac{\partial \mathcal{J}(\boldsymbol{w}_1, \boldsymbol{m}_j, \boldsymbol{w}_2)}{\partial \boldsymbol{w}_1(k)}, \quad (25)$$

where μ_{w_1} and γ_{w_1} are the tuning value and forgetting-factor for $\boldsymbol{w}_1(k)$ and $\zeta_{w_1}(k)$ can be defined by (26)-(28).

$$\zeta_{w_1}(k+1) = \gamma_{w_1} \cdot \zeta_{w_1}(k) - \frac{\beta(k)}{\boldsymbol{x}(k)^T \boldsymbol{x}(k)} \frac{\boldsymbol{w}_2(k)^T \boldsymbol{x}(k)}{\sigma_x} \epsilon(k), \quad (26)$$

$$\beta(k) = \alpha(k)^T \cdot D \cdot \boldsymbol{m}_j(k), \quad (27)$$

$$\gamma_{w_1} = \frac{\varphi_{w_1}(k)^T \cdot \zeta_{w_1}(k)}{\varphi_{w_1}(k+1)^T \cdot \varphi_{w_1}(k)}. \quad (28)$$

where $\alpha(k)$ is given in (12).

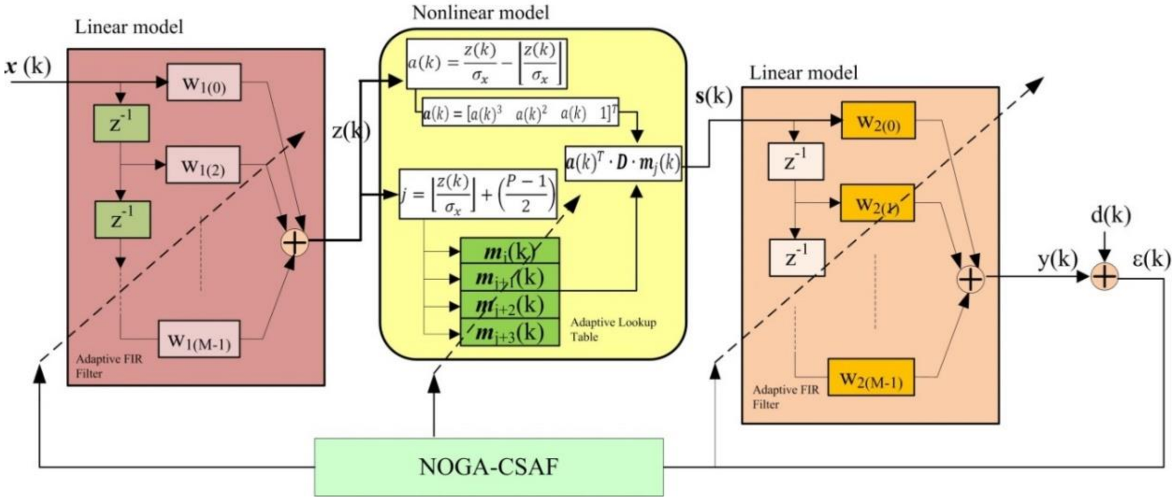

Figure 1. Proposed cascade spline-based adaptive filtering based NOGA algorithm

3. METHOD FOR CONVERGENCE PROPERTIES

The convergence properties of proposed NOGA-CSAF learning algorithm can be verified with the help of error $\epsilon(k+1)$ by Taylor series expansion [6] as shown in (29).

$$\epsilon(k+1) = \epsilon(k) + \delta_{\boldsymbol{w}_2} \cdot \frac{\partial \epsilon(k)}{\partial \boldsymbol{w}_2(k)}\Big|_{\boldsymbol{w}_1, \boldsymbol{m}_j = constant} + \delta_{\boldsymbol{m}_j} \cdot \frac{\partial \epsilon(k)}{\partial \boldsymbol{m}_j(k)}\Big|_{\boldsymbol{w}_1, \boldsymbol{w}_2 = constant} + \delta_{\boldsymbol{w}_1} \cdot \frac{\partial \epsilon(k)}{\partial \boldsymbol{w}_1(k)}\Big|_{\boldsymbol{w}_2, \boldsymbol{m}_j = constant}. \quad (29)$$

All expression terms in (29) can be derived by (30)-(35).

$$\frac{\partial \epsilon(k)}{\partial \boldsymbol{w}_2(k)} = -\frac{\partial y(k)}{\partial \boldsymbol{w}_2(k)} = -\boldsymbol{s}(k), \quad (30)$$

$$\frac{\partial \epsilon(k)}{\partial \boldsymbol{m}_j(k)} = -\frac{\partial y(k)}{\partial \boldsymbol{m}_j(k)} = -\,\boldsymbol{a}(k)^T \cdot \boldsymbol{D} \cdot \boldsymbol{w}_2(k), \quad (31)$$

$$\frac{\partial \epsilon(k)}{\partial \boldsymbol{w}_1(k)} = -\frac{\partial y(k)}{\partial \boldsymbol{w}_1(k)} = -\frac{\beta(k)\boldsymbol{w}_2(k)^T \boldsymbol{x}(k)}{\sigma_x}, \quad (32)$$

$$\delta_{\boldsymbol{w}_2} \approx \mu_{w_2} \cdot \frac{\boldsymbol{s}(k)\epsilon(k)}{\boldsymbol{x}(k)^T \boldsymbol{x}(k)}, \quad (33)$$

$$\delta_{\boldsymbol{m}_j} \approx \mu_{\boldsymbol{m}_j} \cdot \frac{\boldsymbol{a}(k)^T \cdot \boldsymbol{D} \cdot \boldsymbol{w}_2(k)\epsilon(k)}{\boldsymbol{x}(k)^T \boldsymbol{x}(k)}, \quad (34)$$

$$\delta_{\boldsymbol{w}_1} \approx \mu_{w_1} \cdot \frac{\beta(k)}{\sigma_x} \frac{\boldsymbol{w}_2(k)^T \boldsymbol{x}(k)\epsilon(k)}{\boldsymbol{x}(k)^T \boldsymbol{x}(k)}. \quad (35)$$

By substituting (30) - (35) into (29), it is possible to obtain (36).

$$\epsilon(k+1) = \left[1 - \mu_{w_2}\|\boldsymbol{s}(k)\|^2 - \mu_{m_j}\|\,\boldsymbol{a}(k)^T \cdot \boldsymbol{D} \cdot \boldsymbol{w}_2(k)\|^2 - \frac{\mu_{w_1}}{\sigma_x{}^2}\|\beta(k)\boldsymbol{w}_2(k)^T \boldsymbol{x}(k)\|^2\right] \cdot \epsilon(k). \quad (36)$$

We assume that $|\epsilon(k+1) < \epsilon(k)|$ in (36) to certify the convergence, resulting in (37).

$$\left|1 - \mu_{w_2}\|\boldsymbol{s}(k)\|^2 - \mu_{m_j}\|\,\boldsymbol{a}(k)^T \cdot \boldsymbol{D} \cdot \boldsymbol{w}_2(k)\|^2 - \frac{\mu_{w_1}}{\sigma_x{}^2}\|\beta(k)\boldsymbol{w}_2(k)^T \boldsymbol{x}(k)\|^2\right| < 1\,. \quad (37)$$

Referring to (37), the bound on the learning rates can be implied as (38).

$$0 < \mu_{w_2}\|\boldsymbol{s}(k)\|^2 + \mu_{m_j}\|\,\boldsymbol{a}(k)^T \cdot \boldsymbol{D} \cdot \boldsymbol{w}_2(k)\|^2 + \frac{\mu_{w_1}}{\sigma_x{}^2}\|\beta(k)\boldsymbol{w}_2(k)^T \boldsymbol{x}(k)\|^2 < 2\,. \quad (38)$$

It is seen that the proposed NOGA-CSAF approach can be confirmed to converge into its own optimum point when μ_{w_2}, μ_{m_j}, and μ_{w_1} are selected into the bound.

4. EXPERIMENTAL RESULTS AND DISCUSSION

We assume that the identification of unknown CSAF architecture [19] consists of two linear components $\boldsymbol{w}_{2_0}, \boldsymbol{w}_{1_0}$ and the 23-point of a nonlinear function of LUT length of $\boldsymbol{m}_0$ deployed by as (39)-(41).

$$\boldsymbol{w}_{2_0} = [1, 0.5, -0.25, 0.15, 0.25, -0.10, 0.05]^T, \quad (39)$$

$$\boldsymbol{w}_{1_0} = [0.6, -0.4, 0.25, -0.15, 0.1, -0.05, 0.001]^T, \quad (40)$$

$$\boldsymbol{m}_0 = [-2.2, -2.0, -1.8, \cdots, -0.8, -0.91, -0.40, -0.20, 0.05, 0, -0.40, 0.58, \cdots, 2.2]^T. \quad (41)$$

The input signal can be generated by (42).

$$\boldsymbol{x}(k+1) = \lambda \cdot \boldsymbol{x}(k) + \sqrt{1-\lambda^2} \cdot \eta(k), \quad (42)$$

where $0 \leq \lambda < 1$ is a parameter concerned with a level of correlation between connected samples and $\eta(k)$ denotes as a zero-mean white Gaussian noise. For this experiment, λ is set at 0.125 and 0.725 and the 30 dB signal to noise ratio (SNR) is set for the simulation.

Fixed parameters for learning algorithms are as follows: $\mu_{w_1} = 1.25 \times 10^{-3}, \mu_{w_2} = 5.25 \times 10^{-3}$, $\mu_{m_j} = 9.75 \times 10^{-2}$ for proposed NOGA-CSAF approach, $\mu_{w_1} = 1.5 \times 10^{-2}, \mu_{w_2} = 3.90 \times 10^{-2}$, $\mu_{m_j} = 1.40 \times 10^{-2}$ for LMS-CSAF algorithm. The number of tap (*M*) of all cases is 7 and the 3rd degree of spline (*P* = 3) is used. From [25], we assume to initialize $\boldsymbol{w}_1(0) = \boldsymbol{w}_2(0) = [1 \quad 0 \quad \cdots \quad 0]^{\mathrm{T}}$. The basis spline matrix (***D***) named "Catmull–Rom" is used as [8], [26].

$$\boldsymbol{D} = {}^{1}\!/_{2}\begin{bmatrix} -1 & 3 & -3 & 1 \\ 2 & -5 & 4 & -1 \\ -1 & 0 & 1 & 0 \\ 0 & 2 & 0 & 0 \end{bmatrix}. \tag{43}$$

Figure 2 shows the components of two linear adaptive filters $\boldsymbol{w}_2(k)$ in (13) and $\boldsymbol{w}_1(k)$ in (23) from proposed NOGA-CSAF compared to $\boldsymbol{w}_{2_0}$ in (39) and $\boldsymbol{w}_{1_0}$ in (40). Results show that the proposed $\boldsymbol{w}_2(k)$ and $\boldsymbol{w}_1(k)$ can update adaptively. While Figure 3 depicts the adaptive spline controlling vector $\boldsymbol{m}_j(k)$ in (18) compared with the target $\boldsymbol{m}_0$ in (41).

For the nonlinear identification dynamic system [19], a white Gaussian noise random sequence for the uniform noise is used through the 4th order Butterworth of infinite impulse response transfer function for the first linear block filtering is as (44):

$$H_1 = \frac{(0.2851+0.5704z^{-1}+0.2851z^{-2})}{1-0.1024z^{-1}+0.4475z^{-2}} \cdot \frac{(0.2851+0.5701z^{-1}+0.2851z^{-2})}{1-0.0736z^{-1}+0.0408z^{-2}}, \tag{44}$$

and the transfer function of the 4th order Chebyshev IIR filter for the second linear block filtering is as (45).

$$H_2 = \frac{(0.2025+0.2880z^{-1}+0.2025z^{-2})}{1-1.0100z^{-1}+0.5861z^{-2}} \cdot \frac{(0.2025+0.0034z^{-1}+0.2025z^{-2})}{1-0.6591z^{-1}+0.1498z^{-2}}. \tag{45}$$

Then, the nonlinear block is shown by (46).

$$y(k) = \frac{2 \cdot x(k)}{1+|x(k)|^2}. \tag{46}$$

Results of mean square error (MSE) are then computed by (47).

$$MSE(k) = 10\log(d(k) - \boldsymbol{w}_2(k)^T \boldsymbol{s}(k)^2). \tag{47}$$

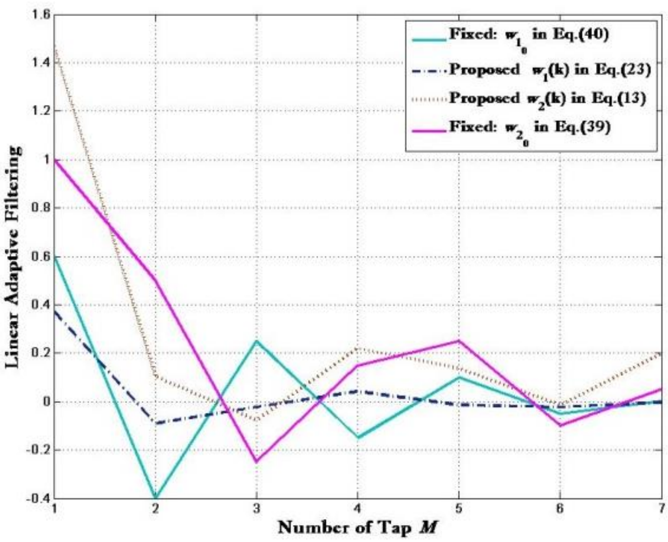

Figure 2. Comparing simulation results of proposed NOGA-CSAF algorithm in the linear components

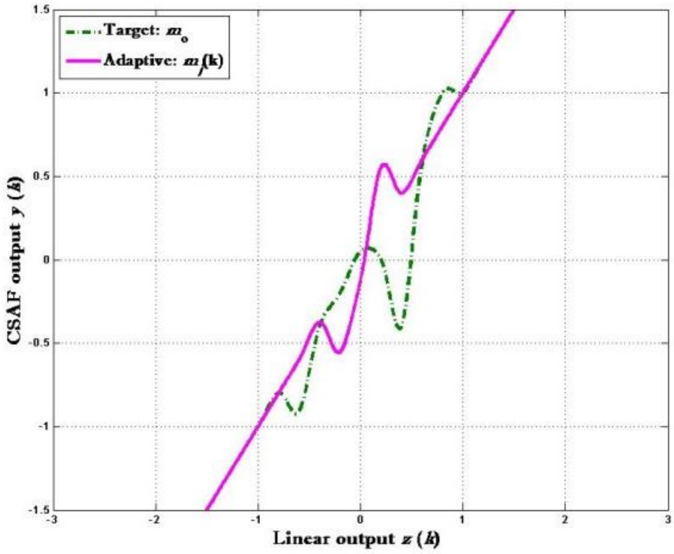

Figure 3. Comparison between the adaptive spline vector $\boldsymbol{m}_j(k)$ and target $\boldsymbol{m}_0$

Figure 4 shows the MSE curves of cascade architecture getting from (47) at λ=0.125 in (42) for proposed NOGA-CSAF are compared with LMS-CSAF [19] in the different step-size parameters averaged from 100 simulations. Figure 5 shows the MSE curves at λ=0.725 in (42) for proposed NOGA-CSAF compared with LMS-CSAF [19] in the different step-size parameters averaged from 100 simulations. In addition, Figures 3 and 4 also depict that proposed NOGA-CSAF can perform clearly the superior results compared to the conventional LMS-CSAF approach with the different step-size values.

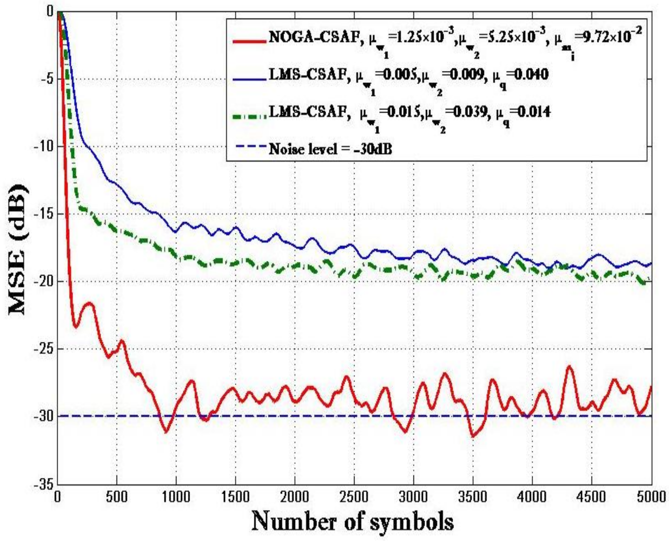

Figure 4. Trends of MSE curves of cascade architecture at λ=0.125 of proposed NOGA-CSAF

Referring to Figures 4 and 5, the results in MSE can confirm the effectiveness of the proposed NOGA-CSAF approach in terms of fast convergence towards the minimized cost function. The averaged MSE of the proposed NOGA-CSAF algorithm compared with the LMS-CSAF is summarized in Table 1. Notice that the proposed algorithm can demonstrate a better performance compared with all cases. It is confirmed that the proposed weight vectors and spline-based controlling coefficient in CSAF model can be changed adaptively by NOGA algorithm during the learning process.

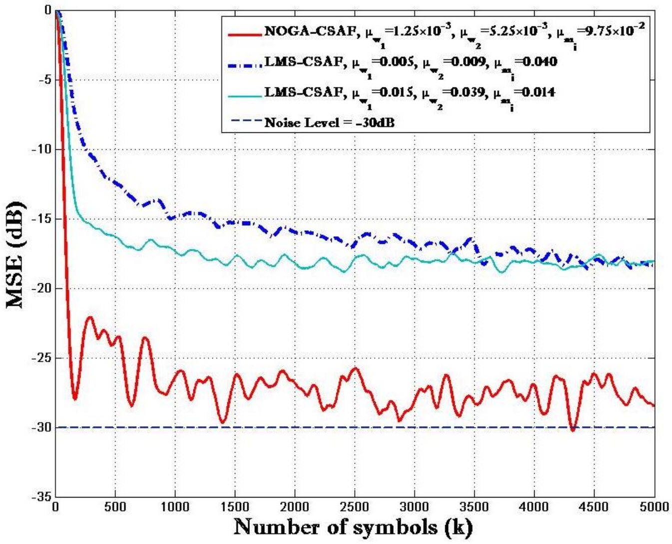

Figure 5. Trends of MSE curves of cascade architecture at λ=0.725 of proposed NOGA-CSAF

Table 1. Averaged MSE in unit of dB of proposed NOGA-CSAF approach

Algorithm	Set-up parameters	Averaged MSE (dB)	
		$\lambda = 0.125$	$\lambda = 0.725$
NOGA-CSAF	$\mu_{w_1} = 1.25 \times 10^{-3}$ $\mu_{w_2} = 5.25 \times 10^{-3}$ $\mu_{m_j} = 9.75 \times 10^{-2}$	**-25.005 dB**	**-21.741 dB**
LMS-CSAF [19]	$\mu_{w_1} = 1.50 \times 10^{-2}$ $\mu_{w_2} = 3.90 \times 10^{-2}$ $\mu_{m_j} = 1.40 \times 10^{-2}$	-18.975 dB	-17.739 dB
LMS-CSAF [19]	$\mu_{w_1} = 5.00 \times 10^{-3}$ $\mu_{w_2} = 9.00 \times 10^{-3}$ $\mu_{m_j} = 4.00 \times 10^{-2}$	-18.371 dB	-17.281 dB

5. CONCLUSION

The cascade architecture of spline adaptive filtering based on NOGA algorithm has been introduced with some modifications of stochastic gradient-based mechanism. Accordingly, CSAF based on NOGA is proposed in this paper. Also, the convergence properties of the proposed NOGA-CSAF have been derived in terms of instantaneous error using Taylor series expansion. Several experiments are conducted and tested in the nonlinear identification system. Results of MSE curves clearly show that NOGA-CSAF outperforms the conventional LMS-CSAF in the case of underlying nonlinear identification system.

REFERENCES

[1] Z. Ma and S. Tong, "Nonlinear filters-based adaptive fuzzy control of strict-feedback nonlinear systems with unknown asymmetric dead-zone output," *IEEE Transactions on Automation Science and Engineering*, pp. 1–11, 2024, doi: 10.1109/TASE.2023.3308528.

[2] G. Qian, D. Luo, and S. Wang, "A robust adaptive filter for a complex hammerstein system," *Entropy*, vol. 21, no. 2, Feb. 2019, doi: 10.3390/e21020162.

[3] G. Cheng, L. Liao, H. Chen, and J. Lu, "Semi-blind source separation for nonlinear acoustic echo cancellation," *IEEE Signal Processing Letters*, vol. 28, pp. 474–478, 2021, doi: 10.1109/LSP.2021.3060325.

[4] J. Jiang, V. Vijayarajan, and L. Tan, "Channel sparsity aware function expansion filters using the RLS algorithm for nonlinear acoustic echo cancellation," *IEEE Access*, vol. 8, pp. 118305–118314, 2020, doi: 10.1109/ACCESS.2020.3005408.

[5] S. Guan and B. Biswal, "Spline adaptive filtering algorithm based on different iterative gradients: Performance analysis and comparison," *Journal of Automation and Intelligence*, vol. 2, no. 1, pp. 1–13, Feb. 2023, doi: 10.1016/j.jai.2022.100008.

[6] M. Scarpiniti, D. Comminiello, R. Parisi, and A. Uncini, "Spline adaptive filters," in *Adaptive Learning Methods for Nonlinear System Modeling*, Elsevier, 2018, pp. 47–69.

[7] T. Paireder, C. Motz, and M. Huemer, "Spline-based adaptive cancellation of even-order Intermodulation distortions in LTE-A/5G RF transceivers," *IEEE Transactions on Vehicular Technology*, vol. 70, no. 6, pp. 5817–5832, Jun. 2021, doi: 10.1109/TVT.2021.3076843.

[8] M. Scarpiniti, D. Comminiello, and A. Uncini, "Convex combination of spline adaptive filters," in *2019 27th European Signal Processing Conference (EUSIPCO)*, Sep. 2019, pp. 1–5, doi: 10.23919/EUSIPCO.2019.8903134.

[9] W. Wang, H. Zhao, X. Zeng, and K. Dogancay, “Steady-state performance analysis of nonlinear spline adaptive filter under maximum correntropy criterion,” *IEEE Transactions on Circuits and Systems II: Express Briefs*, vol. 67, no. 6, pp. 1154–1158, Jun. 2020, doi: 10.1109/TCSII.2019.2929536.

[10] S. Sitjongsataporn and W. Chimpat, “Adaptive step-size normalised least mean square algorithm for spline adaptive filtering,” in *2019 34th International Technical Conference on Circuits/Systems, Computers and Communications (ITC-CSCC)*, Jun. 2019, pp. 1–4, doi: 10.1109/ITC-CSCC.2019.8793383.

[11] C. Liu, Z. Zhang, and X. Tang, “Sign normalized Hammerstein spline adaptive filtering algorithm in an impulsive noise environment,” *Neural Processing Letters*, vol. 50, no. 1, pp. 477–496, Aug. 2019, doi: 10.1007/s11063-019-09996-6.

[12] H. Zhao, Y. Gao, and R. Zhu, “Least mean p-power Hammerstein spline adaptive filtering algorithm: formulation and analysis,” *IEEE Transactions on Aerospace and Electronic Systems*, pp. 1–9, 2024, doi: 10.1109/TAES.2024.3403073.

[13] S. Sitjongsataporn, “Diffusion Hammerstein spline adaptive filtering based on orthogonal gradient adaptive algorithm,” *IEEE Access*, vol. 10, pp. 57398–57412, 2022, doi: 10.1109/ACCESS.2022.3179421.

[14] S. Sitjongsataporn and P. Nurarak, “Normalised least mean fourth algorithm for Hammerstein spline adaptive filtering,” in *TENCON 2023 - 2023 IEEE Region 10 Conference (TENCON)*, Oct. 2023, pp. 1008–1011, doi: 10.1109/TENCON58879.2023.10322381.

[15] Y. Qian, X. Huo, Q. Liu, J. Liu, and H. Zhao, “Equivalent circuit-based modeling of ultrasonic motors for Hammerstein systems,” in *2023 IEEE 12th Data Driven Control and Learning Systems Conference (DDCLS)*, May 2023, pp. 1568–1572, doi: 10.1109/DDCLS58216.2023.10167098.

[16] L. Anttila *et al.*, “Full-duplexing with SDR devices: algorithms, FPGA implementation, and real-time results,” *IEEE Transactions on Wireless Communications*, vol. 20, no. 4, pp. 2205–2220, Apr. 2021, doi: 10.1109/TWC.2020.3040226.

[17] P. P. Campo, D. Korpi, L. Anttila, and M. Valkama, “Nonlinear digital cancellation in full-duplex devices using spline-based hammerstein model,” in *2018 IEEE Globecom Workshops (GC Wkshps)*, Dec. 2018, pp. 1–7, doi: 10.1109/GLOCOMW.2018.8644362.

[18] K. Samiee and P. Kovacs, “ECG decomposition using cascaded spline projection residual auto encoders,” in *2023 Computing in Cardiology (CinC)*, Nov. 2023, pp. 1–4, doi: 10.22489/CinC.2023.227.

[19] M. Scarpiniti, D. Comminiello, R. Parisi, and A. Uncini, “Novel cascade spline architectures for the identification of nonlinear systems,” *IEEE Transactions on Circuits and Systems I: Regular Papers*, vol. 62, no. 7, pp. 1825–1835, Jul. 2015, doi: 10.1109/TCSI.2015.2423791.

[20] P. Pascual Campo, L. Anttila, D. Korpi, and M. Valkama, “Cascaded spline-based models for complex nonlinear systems: methods and applications,” *IEEE Transactions on Signal Processing*, vol. 69, pp. 370–384, 2021, doi: 10.1109/TSP.2020.3046355.

[21] S. Sitjongsataporn, “Cascade spline adaptive filtering based on normalised least mean square algorithm,” in *2023 International Conference on Power, Energy and Innovations (ICPEI)*, Oct. 2023, pp. 76–79, doi: 10.1109/ICPEI58931.2023.10473855.

[22] D. P. Sergio and R. Diniz, *Adaptive filtering: algorithms and practical implementation*. 2002.

[23] S. Sitjongsataporn, “Convergence analysis of greedy normalised orthogonal gradient adaptive algorithm,” in *2018 18th International Symposium on Communications and Information Technologies (ISCIT)*, Sep. 2018, pp. 345–348, doi: 10.1109/ISCIT.2018.8587855.

[24] D. E. Lee, K. Nakamura, J.-H. Tak, and B.-W. Hong, “A continual learning algorithm based on orthogonal gradient descent beyond neural tangent Kernel regime,” *IEEE Access*, vol. 11, pp. 85395–85404, 2023, doi: 10.1109/ACCESS.2023.3303869.

[25] S. S. Haykin, *Adaptive filter theory*. Pearson Education India, 2002.

[26] Z. Qiao, Z. Yu, H. Yin, and S. Shen, “Online monocular lane mapping using Catmull-Rom spline,” in *2023 IEEE/RSJ International Conference on Intelligent Robots and Systems (IROS)*, Oct. 2023, pp. 7179–7186, doi: 10.1109/IROS55552.2023.10341707.

BIOGRAPHIES OF AUTHORS

Theerayod Wiangtong received the B.Eng. degree (First-class honors) in electronic engineering from King Mongkut’s Institute of Technology Ladkrabang, the M.Sc. degree in satellite communication from University of Surrey, and the PhD. degree in digital system design, co-design from Imperial College, London, UK. Currently, he is an associate professor with the Department of Electrical Engineering, King Mongkut’s Institute of Technology Ladkrabang. His research interests include digital IC design, hardware/software co-design, embedded systems, algorithm and optimization, and data processing. He can be contacted at theerayod.wi@kmitl.ac.th.

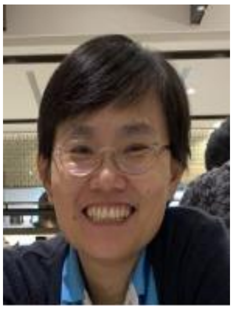

Suchada Sitjongsataporn received the B.Eng. degree (First-class honors) and D.Eng. degree in electronic engineering from Mahanakorn University of Technology, Bangkok, Thailand in 2002 and 2009. She has worked as lecturer at the Department of Electronic Engineering, Mahanakorn University of Technology since 2002. Currently, she is an associate professor in electronic engineering and the assistant president for research in Mahanakorn University of Technology. Her research interests are mathematical and statistical models in the area of adaptive signal processing for communications, networking, embedded system, machine learning, image and video processing. She can be contacted at email: ssuchada@mut.ac.th.